SUPPLEMENTARY DATA FOR:

Resensitising proteasome inhibitor-resistant myeloma with sphingosine kinase 2 inhibition

Melissa K. Bennett[1], Manjun Li[1], Melinda N. Tea[1], Melissa R. Pitman[1,2], John Toubia[1,3], Paul P.-S. Wang[1,3], Dovile Anderson[4], Darren J. Creek[4], Robert Z. Orlowski[5], Briony L. Gliddon[1], Jason A. Powell[1,6], Craig T. Wallington-Beddoe[1,6,7,8,*] and Stuart M. Pitson[1,2,6,*]

[1] Centre for Cancer Biology, University of South Australia and SA Pathology, Bradley Building, North Tce, Adelaide SA, 5000, Australia;
[2] School of Biological Sciences, University of Adelaide, Adelaide SA, 5000, Australia
[3] ACRF Cancer Genomics Facility, Centre for Cancer Biology, SA Pathology, Adelaide, South Australia, 5000, Australia;
[4] Drug Delivery, Disposition and Dynamics, Monash Institute of Pharmaceutical Sciences, Monash University, Parkville, Victoria, Australia
[5] Department of Lymphoma and Myeloma, The University of Texas M.D. Anderson Cancer Center, Houston, TX 77030, USA;
[6] Adelaide Medical School, University of Adelaide, Adelaide SA, 5000, Australia;
[7] College of Medicine and Public Health, Flinders University, Bedford Park SA, 5042, Australia;
[8] Flinders Medical Centre, Bedford Park SA, 5042, Australia
* Authors for correspondence:
Stuart M Pitson, Centre for Cancer Biology, University of South Australia, North Terrace, Adelaide, 5000, Australia; email: stuart.pitson@unisa.edu.au; Tel: +618 8302 7832
Craig T. Wallington-Beddoe, College of Medicine and Public Health, Flinders University, Bedford Park SA, 5042, Australia; email: craig.wallingtonbeddoe@flinders.edu.au; Tel: +618 8204 2831

Supplementary Figure 1

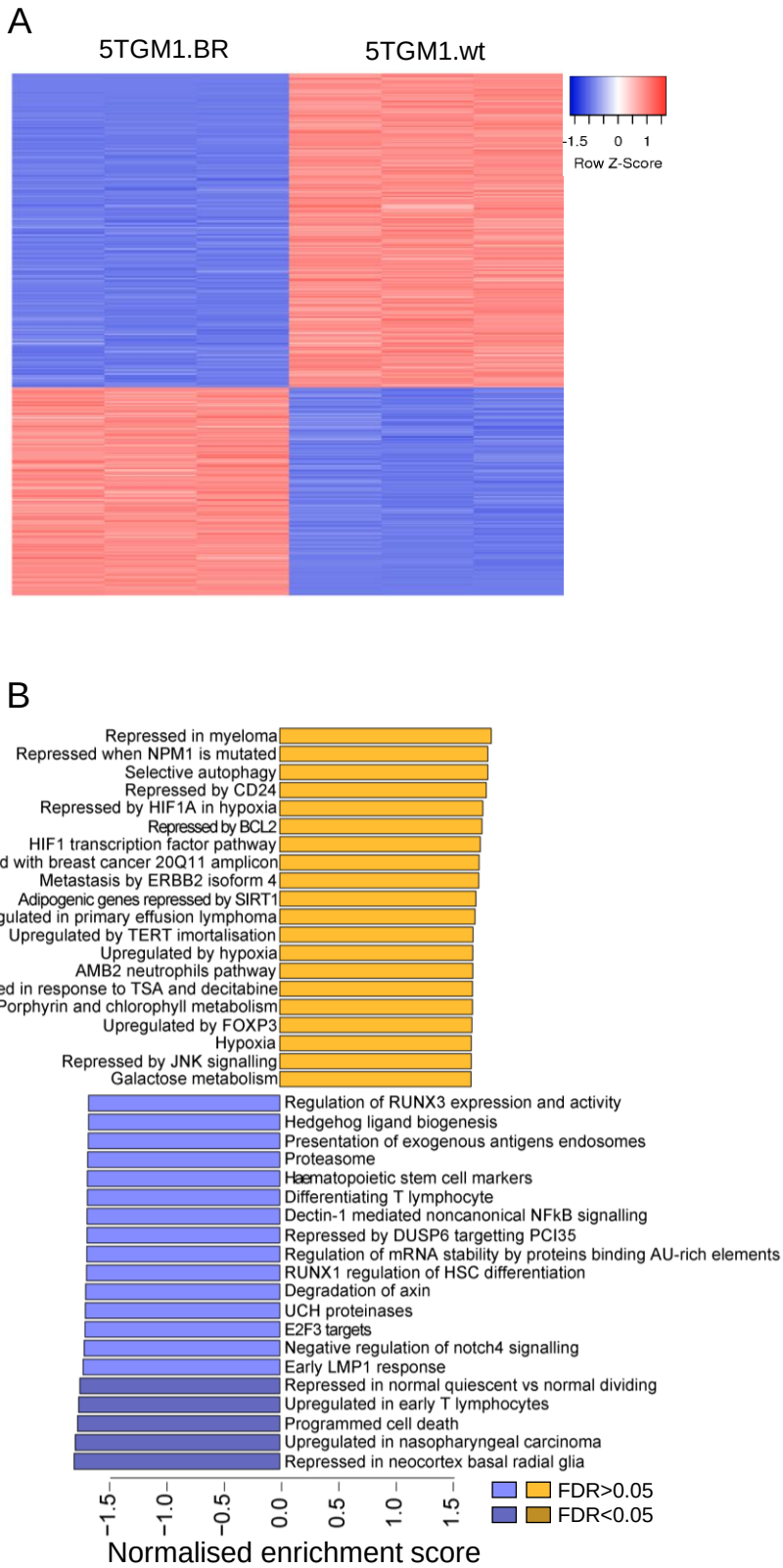

C

Upregulated				Downregulated			
Name	NES	P-value	FDR q-value	Name	NES	P-value	FDR q-value
Boylan Multiple myeloma C D down	1.846	0.000	0.060	Florio Neocortex basal radial glia down	-1.796	0.000	0.015
Mullighan NPM1 mutated signature down	1.817	0.000	0.077	Sengupta Nasopharyngeal carcinoma up	-1.785	0.000	0.012
Reactome Selective autophagy	1.817	0.000	0.052	Reactome Programmed cell death	-1.766	0.000	0.027
Sagiv CD24 targets down	1.803	0.000	0.052	Lee Early T lymphocyte up	-1.755	0.000	0.029
Gross Hypoxia via HIF1A down	1.772	0.000	0.091	Graham Normal quiescent vs normal dividing down	-1.754	0.000	0.036
Vanasse BCL2 targets down	1.766	0.000	0.092	Dirmeier LMP1 response early	-1.716	0.000	0.068
PID HIF1 transcription factor pathway	1.750	0.003	0.114	Reactome Negative regulation of Notch4 signalling	-1.706	0.000	0.077
Nikolsky Breast cancer 20Q11 amplicon	1.740	0.000	0.126	Kong E2F3 targets	-1.698	0.000	0.089
Pedersen Metastasis by ERBB2 isoform 4	1.738	0.002	0.118	Reactome UCH proteinases	-1.697	0.000	0.081
Wang Adipogenic genes repressed by SIRT1	1.714	0.006	0.182	Reactome Degradation of axin	-1.694	0.003	0.079
Klein Primary effusion lymphoma up	1.705	0.004	0.198	Reactome RUNX1 regulates genes involved in differentiation of HSCs	-1.686	0.000	0.088
Kang Immortalised by TERT up	1.688	0.000	0.254	Reactome Regulation of mRNA stability by proteins that bind AU-rich elements	-1.683	0.000	0.087
Elvidge Hypoxia up	1.686	0.000	0.240	Furukawa DUSP6 targets PCI35 down	-1.682	0.000	0.082
PID AMB2 neutrophils pathway	1.686	0.002	0.224	Reactome Dectin-1 mediated noncanonical NFkB signalling	-1.680	0.000	0.080
Kim response to TSA and decitabine up	1.684	0.002	0.219	Lee Differentiating T lymphocyte	-1.680	0.000	0.076
KEGG Porphyrin and chlorophyll metabolism	1.683	0.002	0.209	Park Haematopoietic stem cell markers	-1.678	0.000	0.075
Marson FOXP3 targets stimulated up	1.678	0.011	0.215	KEGG Proteasome	-1.676	0.000	0.073
Qi Hypoxia	1.673	0.003	0.220	Reactome Cross presentation of soluble exogenous antigens endosomes	-1.673	0.002	0.076
Han JNK signalling down	1.673	0.006	0.209	Reactome Hedgehog ligand binding	-1.670	0.002	0.079
KEGG galactose metabolism	1.671	0.002	0.208	Reactome Regulation of RUNX3 expression and activity	-1.669	0.002	0.077

D

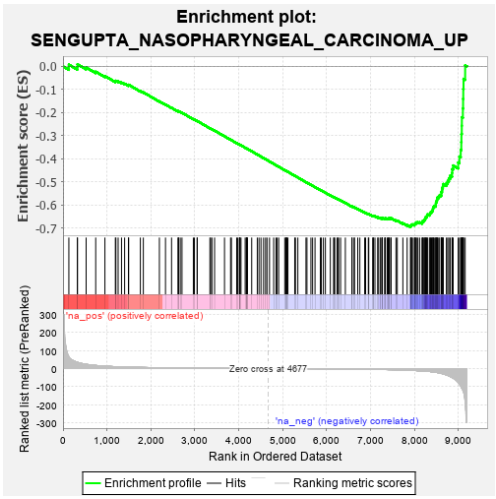
Enrichment plot:
SENGUPTA_NASOPHARYNGEAL_CARCINOMA_UP
Enrichment score (ES)
Ranked list metric (PreRanked)
'na_pos' (positively correlated)
'na_neg' (negatively correlated)
Zero cross at 4677
Rank in Ordered Dataset
Enrichment profile
Hits
Ranking metric scores

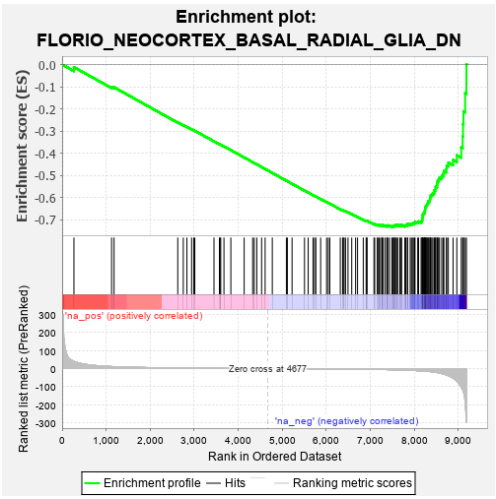
Enrichment plot:
FLORIO_NEOCORTEX_BASAL_RADIAL_GLIA_DN
Enrichment score (ES)
Ranked list metric (PreRanked)
'na_pos' (positively correlated)
'na_neg' (negatively correlated)
Zero cross at 4677
Rank in Ordered Dataset
Enrichment profile
Hits
Ranking metric scores

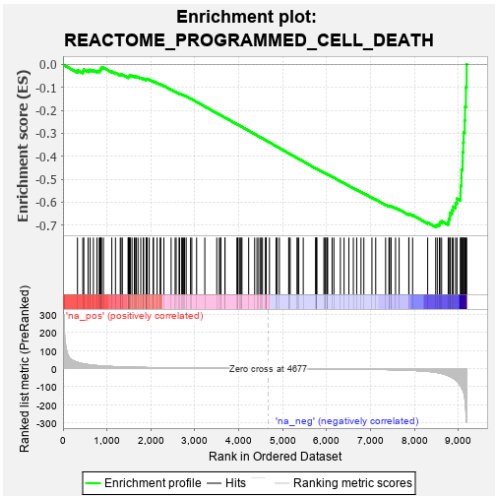
Enrichment plot:
REACTOME_PROGRAMMED_CELL_DEATH
Enrichment score (ES)
Ranked list metric (PreRanked)
'na_pos' (positively correlated)
'na_neg' (negatively correlated)
Zero cross at 4677
Rank in Ordered Dataset
Enrichment profile
Hits
Ranking metric scores

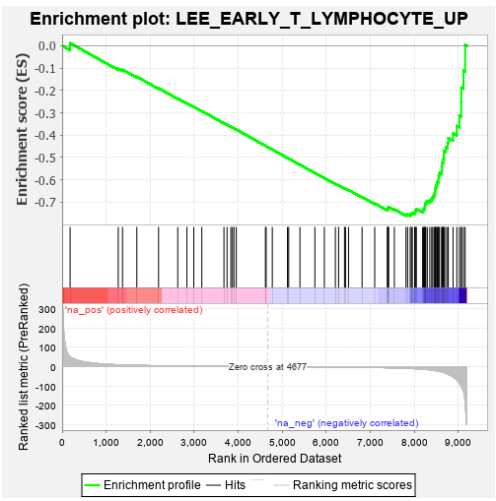
Enrichment plot: LEE_EARLY_T_LYMPHOCYTE_UP
Enrichment score (ES)
Ranked list metric (PreRanked)
'na_pos' (positively correlated)
'na_neg' (negatively correlated)
Zero cross at 4677
Rank in Ordered Dataset
Enrichment profile
Hits
Ranking metric scores

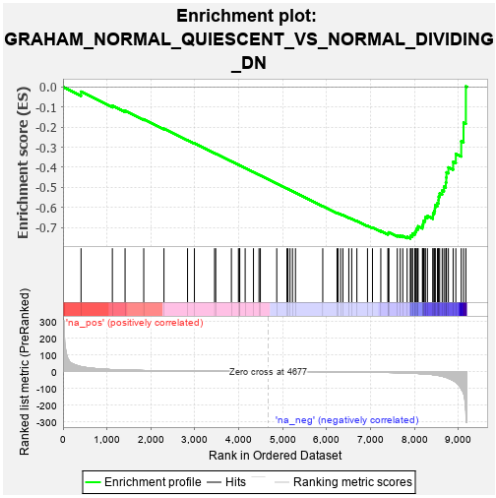
Enrichment plot:
GRAHAM_NORMAL_QUIESCENT_VS_NORMAL_DIVIDING
_DN
Enrichment score (ES)
Ranked list metric (PreRanked)
'na_pos' (positively correlated)
'na_neg' (negatively correlated)
Zero cross at 4677
Rank in Ordered Dataset
Enrichment profile
Hits
Ranking metric scores

Supplementary Figure 1: **RNAseq and gene set enrichment analysis of genes differentially expressed in 5TGM1.BR compared to 5TGM1.wt. A**) RNA-sequencing was performed on 5TGM1.wt and 5TGM1.BR cells, with heat map showing changes in gene expression of at least two-fold between these cells. **B**) Gene set enrichment analysis of differentially regulated genes, with the top twenty upregulated and downregulated pathways shown, with further detail shown in panel (**C**), including the full name of the gene set according to the C2 collection of the Molecular Signature Database, the normalised enrichment score (NES), the nominal p-value, and the false discovery rate (FDR) q-value. **D**) Enrichment plots for gene sets with a false discovery rate of <0.05.

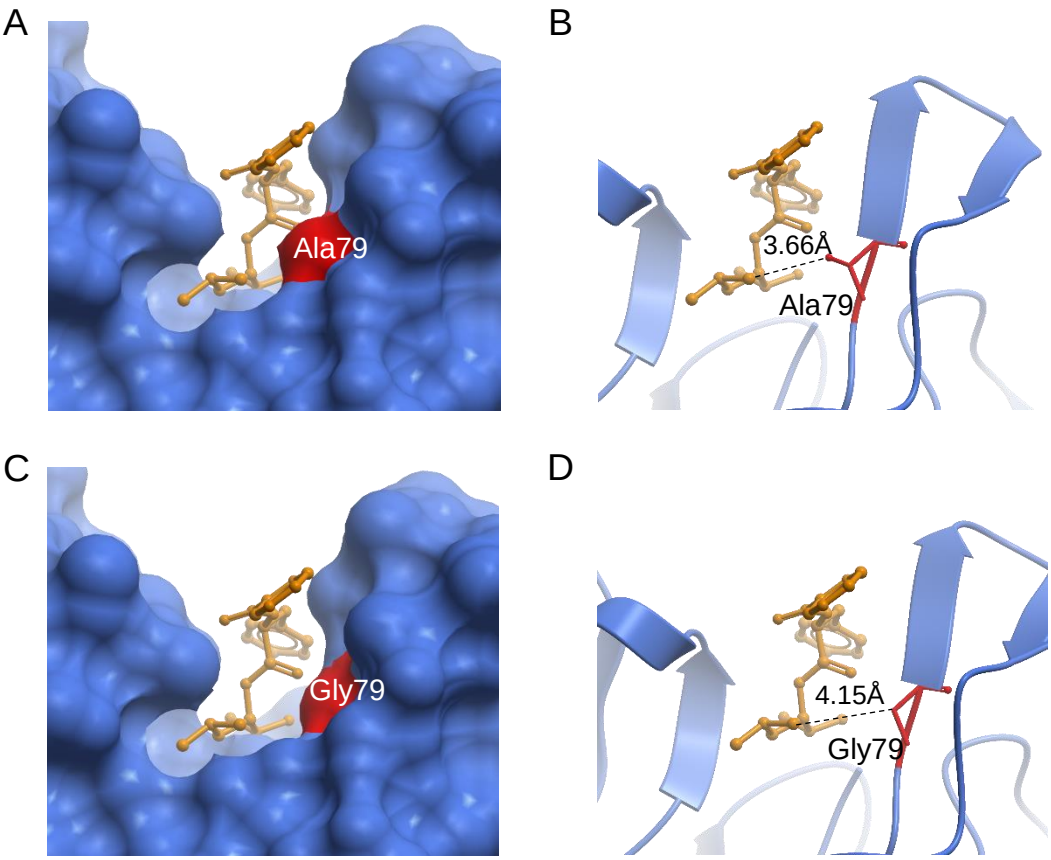

Supplementary Figure 2: **Mutation of Ala79 alters hydrophobic interactions with bortezomib.** The chymotrypsin binding pocket of human PSMB5 crystallised with Bortezomib were analysed using ICM-Pro. PSMB5 crystallised with bortezomib (orange sticks, pdb code: 5lf3_K) is represented in surface view (**A**) or ribbon view (**B**). Ala79 was mutated to Glycine *in silico* (**C**,**D**). Ala79 or the mutated Gly79 are highlighted in red. Distances between the conserved methyl moiety of the inhibitors and side-chain methyl of Ala or alpha carbon of Gly79 were measured and depicted as dashed lines. The Ala79→Gly mutation is not predicted to alter hydrogen bonding interactions in the pocket.

Supplementary Figure 3

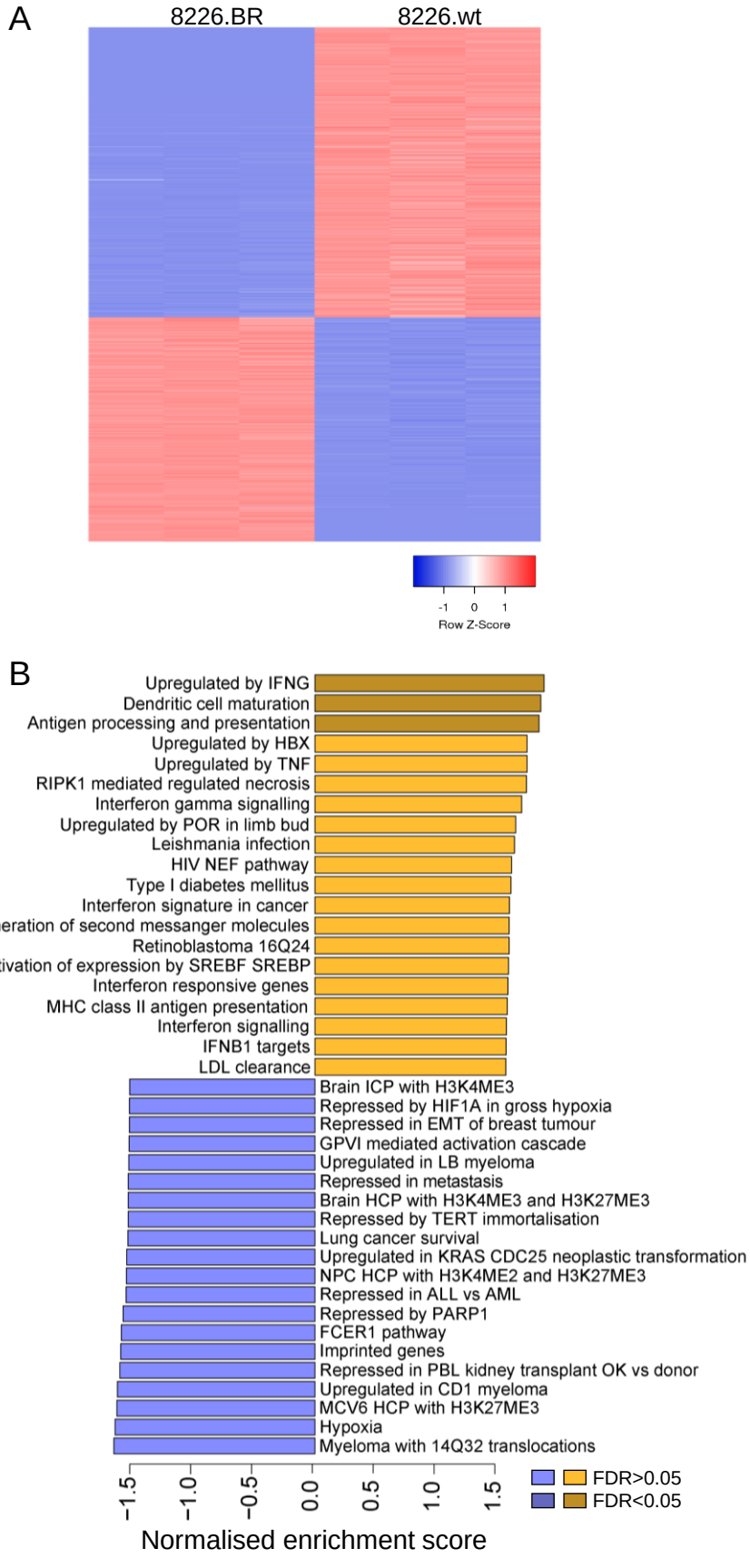

C

Upregulated				Downregulated			
Name	NES	P-value	FDR q-value	Name	NES	P-value	FDR q-value
Sana Response to IFNG up	1.882	0.000	0.025	Mattioli Multiple myeloma with 14Q32 translocations	-1.653	0.000	0.239
Lindstedt Dendritic cell maturation A	1.855	0.000	0.025	Harris hypoxia	-1.643	0.000	0.157
KEGG Antigen processing and presentation	1.841	0.000	0.021	Mikkelsen MCV6 HCP with H3K27ME3	-1.629	0.000	0.165
Wu HBX Targets 2 up	1.743	0.000	0.141	Zhan Multiple myeloma CD1 up	-1.624	0.001	0.149
Sana TNF signalling up	1.742	0.000	0.114	Flechner PBL kidney transplant OK vs donor down	-1.604	0.001	0.225
Reactome RIPK1 mediated regulated necrosis	1.738	0.007	0.106	Brideau Imprinted genes	-1.596	0.002	0.238
Reactome Interferon gamma signalling	1.698	0.000	0.197	0.000P0.543ID FCER1 pathway	-1.592	0.003	0.223
Schmidt POR targets in limb bud up	1.649	0.000	0.416	Simbulan PARP1 targets down	-1.577	0.006	0.302
KEGG Leishmania infection	1.638	0.004	0.435	Golub ALL vs AML down	-1.552	0.003	0.513
PID HIV NEF pathway	1.615	0.009	0.557	Meissner NPC HCP with H3K4ME3 and H3K27ME3	-1.550	0.003	0.484
KEGG Type I diabetes mellitus	1.610	0.012	0.547	Chiaradonna Neoplastic transformation KRAS CDC25 up	-1.548	0.000	0.468
Einav Interferon signature in cancer	1.598	0.009	0.584	Chen Lung cancer survival	-1.539	0.002	0.526
Reactome Generation of second messenger molecules	1.596	0.005	0.561	Lindvall Immortalised by TERT down	-1.536	0.006	0.523
Gratias Retinoblastoma 16Q24	1.594	0.013	0.530	Meissner Brain HCP with H3K4ME3 and H3K27ME3	-1.535	0.000	0.491
Reactome Activation of gene expression by SREBF SREBP	1.590	0.004	0.521	Jaeger Metastasis down	-1.535	0.004	0.464
Browne Interferon responsive genes	1.586	0.004	0.516	Zhan Multiple myeloma LB up	-1.531	0.004	0.469
Reactome MHC class II antigen presentation	1.580	0.000	0.525	Reactome GPVI mediated activation cascade	-1.527	0.006	0.486
Reactome Interferon signalling	1.573	0.000	0.543	Hollern EMT breast tumour down	-1.525	0.004	0.475
Hecker IFNB1 targets	1.570	0.011	0.534	Gross Hypoxia via HIF1A down	-1.524	0.003	0.457
Reactome LDL clearance	1.569	0.012	0.512	Meissner Brain ICP with H3K4ME3	-1.523	0.005	0.448

D

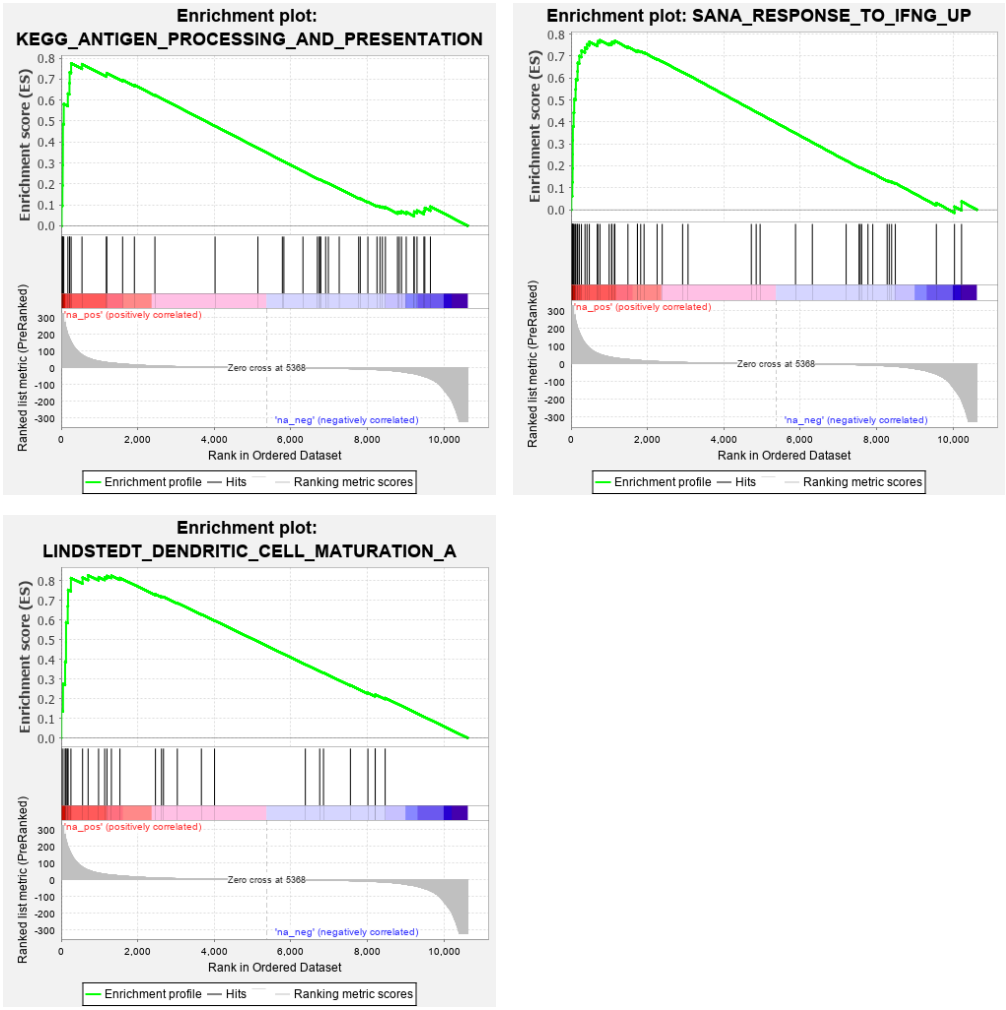

Supplementary Figure 3: **RNAseq and gene set enrichment analysis of genes differentially expressed in 8226.BR compared to 8226.wt. A**) RNA-sequencing was performed on 8226.wt and 8226.BR cells, with the heat map showing changes in gene expression of at least two-fold between these cells. **B**) Gene set enrichment analysis of differentially regulated genes, with the top twenty upregulated and downregulated pathways shown, with further details shown in panel (**C**), including the full name of the gene set according to the C2 collection of the Molecular Signature Database, the normalised enrichment score (NES), the nominal p-value, and the false discovery rate (FDR) q-value. **D**) Enrichment plots for gene sets with a false discovery rate of <0.05.

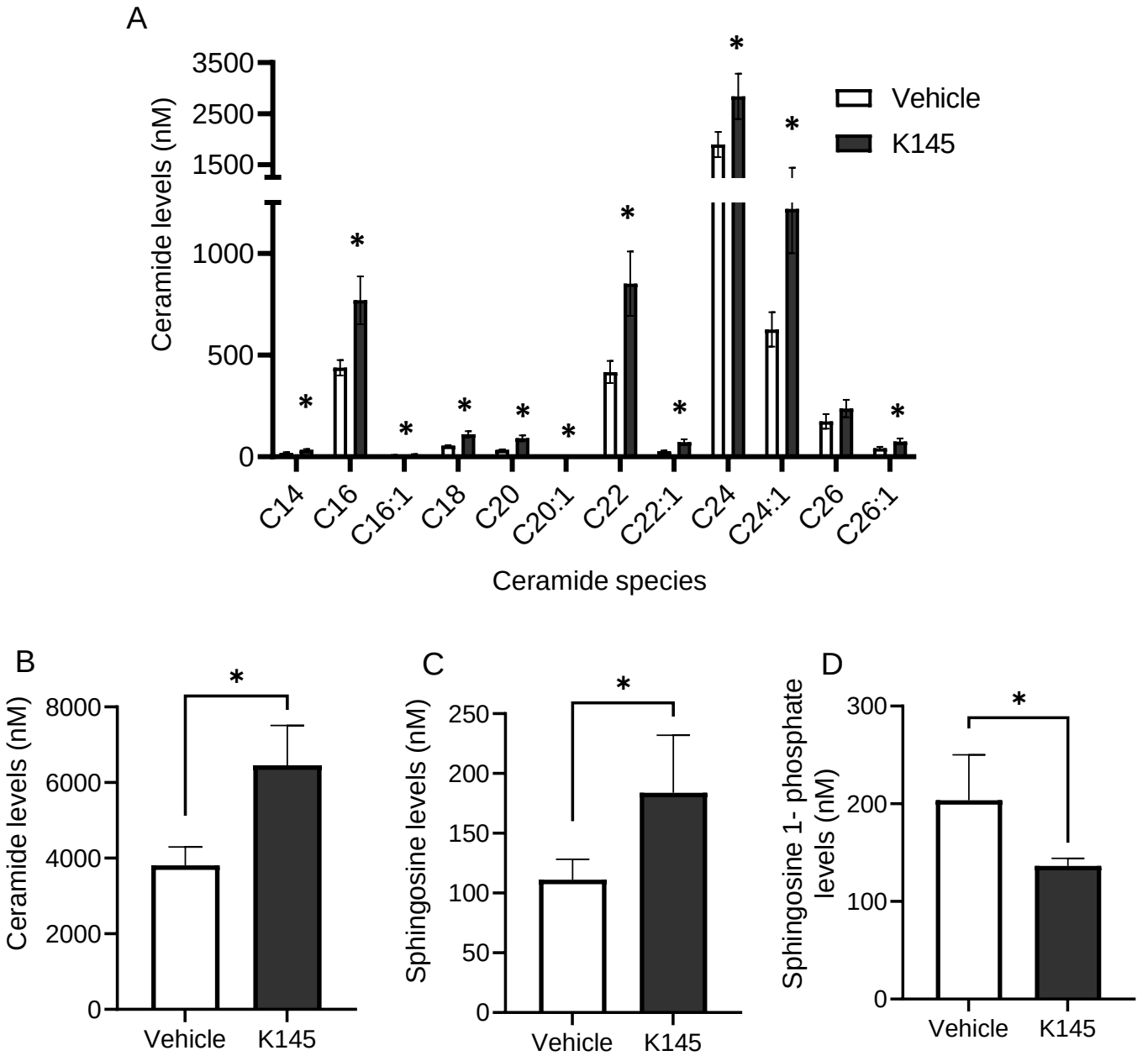

Supplementary Figure 4: **Treatment with K145 increases ceramide and sphingosine, and decreases sphingosine 1 phosphate in bortezomib-resistant myeloma cells.** 5TGM1.BR cells were treated with vehicle or 8 μM K145 for 6h in quadruplicate, and sphingolipidomic analysis performed. **(A)** Levels of individual ceramides species within each sample, with species delineated by length of the N-linked acyl chain. **B)** Total ceramide levels within each sample. **C)** Sphingosine (C18) levels within each sample. **D)** Sphingosine 1-phosphate (C18) levels within each sample. * $p < 0.05$

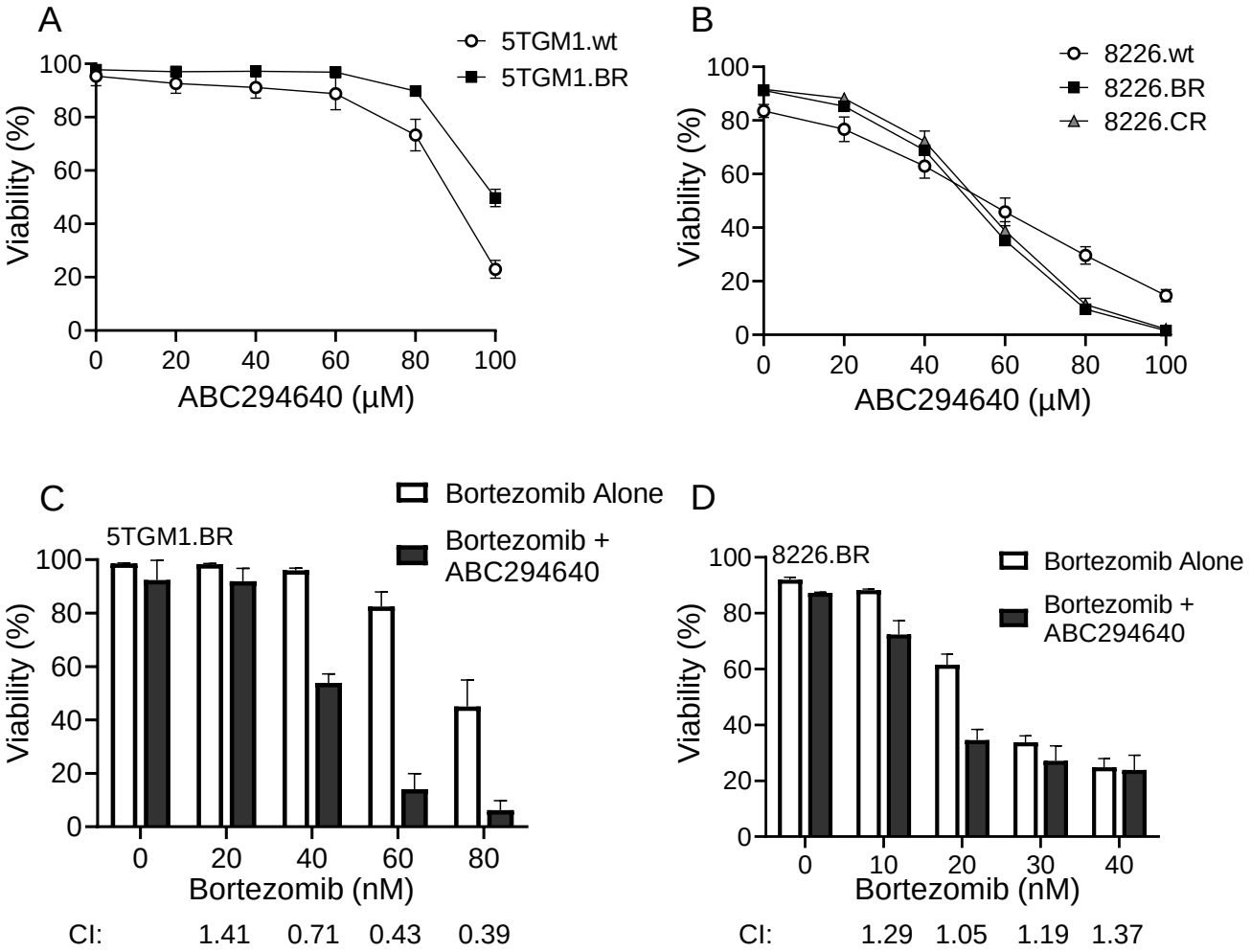

Supplementary Figure 5: **A second SK2 inhibitor ABC294640 largely mimics the effect of K145 on proteasome inhibitor resistant myeloma A)** 5TGM1.wt and 5TGM1.BR cells were treated with increasing concentrations of ABC294640 for 48h, and viability was then assessed by flow cytometry using Annexin-V and PI staining. The EC_{50} for 5TGM1.wt cells was 90.7μM (95% CI 88.5μM-93μM), and the EC_{50} for 5TGM1.BR cells was >100μM (predicted to be 100.4 μM). **B)** 8226.wt, 8226.BR and 8226.CR cells were treated with increasing concentrations of ABC294640 for 48h, and then viability was assessed by flow cytometry, with EC_{50}'s of 66.6μM (95% CI 59.9μM-72.5μM), 55μM (95% CI 53.1μM-56.8μM), and 56.2μM (95% CI 53.8μM-58.7μM) respectively **C)** 5TGM1.BR cells were treated with increasing concentrations of bortezomib with and without 50μM ABC924640 for 48h, and then cell viability was assessed by flow cytometry. **D)** 8226.BR cells were treated with increasing concentrations of bortezomib with and without 20μM ABC294640 for 48h, and then cell viability was assessed by flow cytometry. All data shown represent the mean ± SD of three independent experiments. Combination index (CI) values were calculated using CompuSyn, where a CI of <1 indicates synergy.

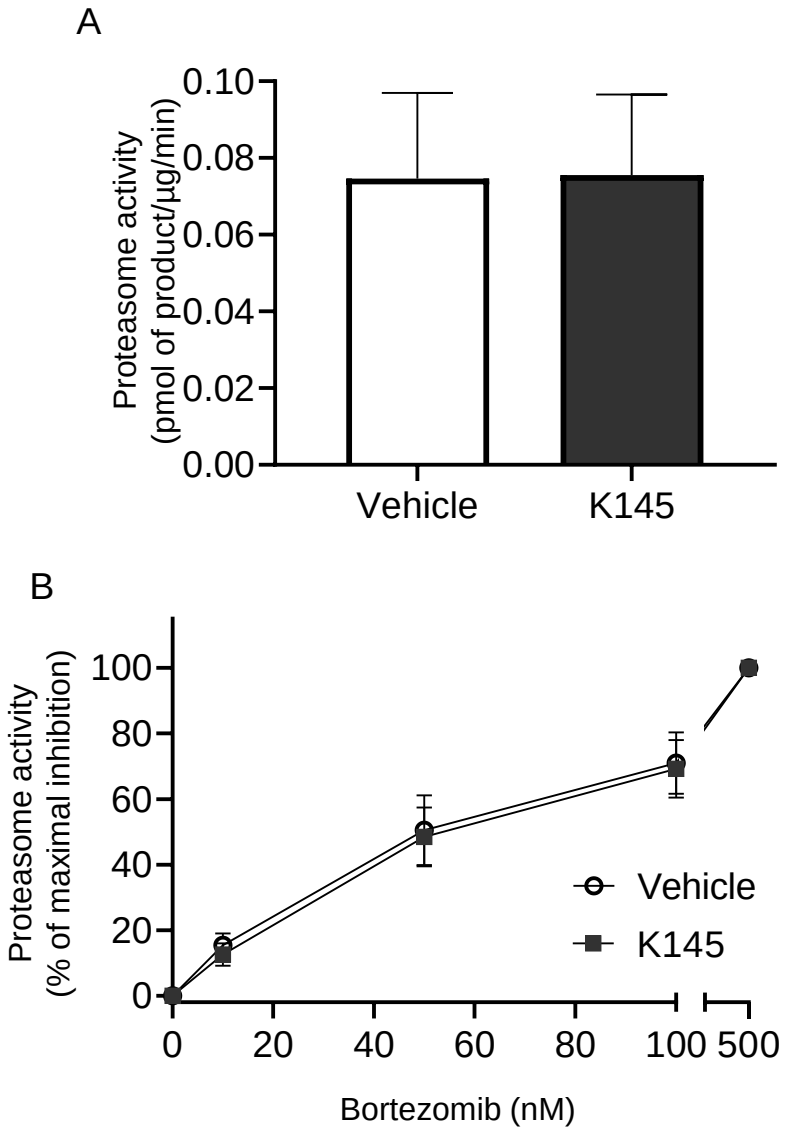

Supplementary Figure 6: **K145 pre-treatment does not change proteasome activity. A)** 5TGM1.BR cells were treated with vehicle or 8µM K145 for 6h. Cell lysates were collected, and chymotrypsin-like activity of the proteasome measured by cleavage of the fluorescent substrate suc-LLVY-AMC. Activity is shown as pmol of suc-LLVY-AMC cleaved per µg protein per min. Data shown represents mean ± SD of three independent experiments. **B)** Proteasome activity measured as in A) with increasing concentrations of bortezomib. Activity shown as a percent of maximal inhibition normalised to control, and is the mean ± SD of three independent experiments.

Supplementary Figure 7

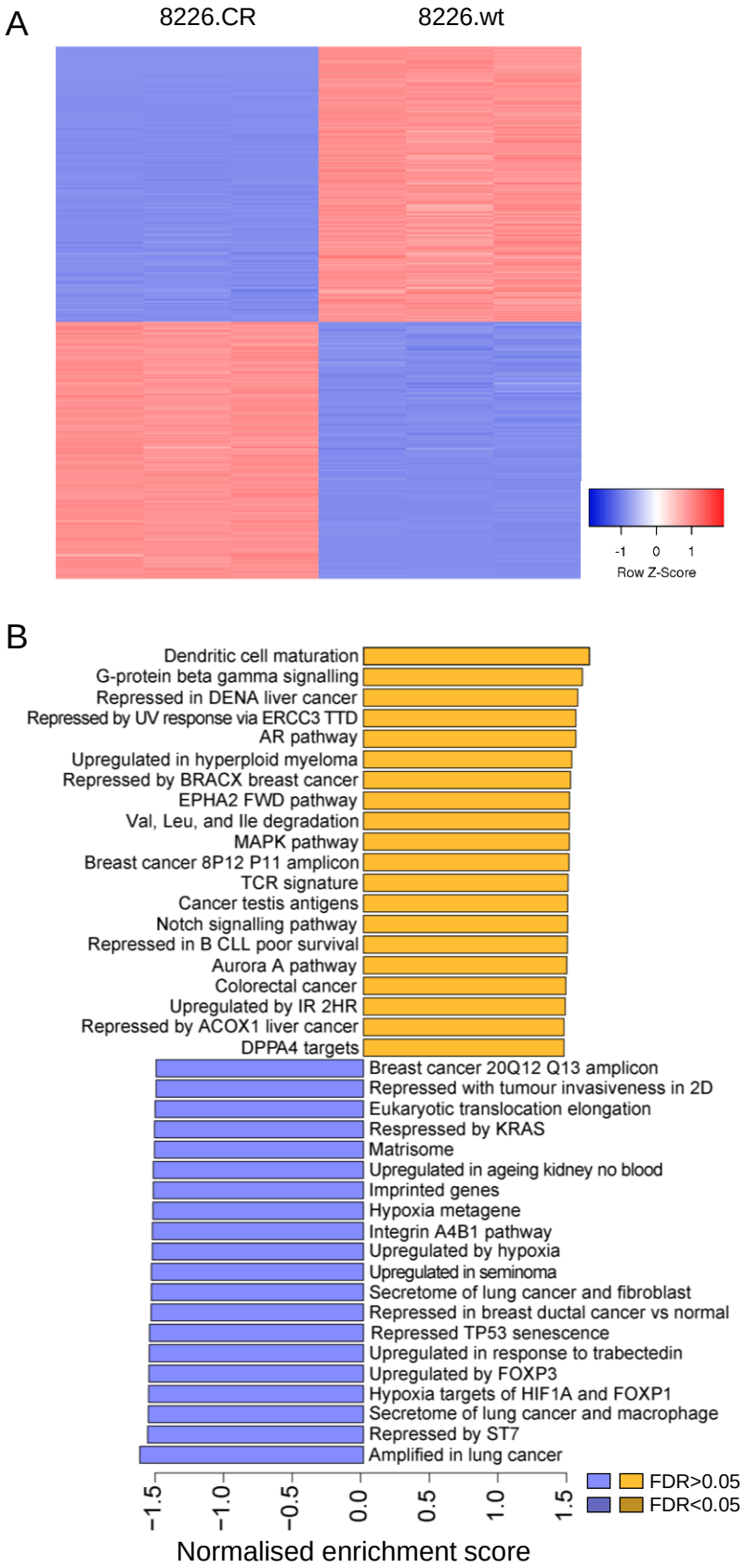

C

Upregulated				Downregulated			
Name	NES	P-value	FDR q-value	Name	NES	P-value	FDR q-value
Lindstedt Dendritic cell maturation A	1.647	0.007	1.0	Li Amplified in lung cancer	-1.632	0.000	0.523
Reactome G protein beta gamma signalling	1.595	0.000	1.0	Hooi ST7 targets down	-1.574	0.005	1.0
Lee Liver cancer DENA down	1.561	0.002	1.0	Zhong Secretome of lung cancer and macrophage	-1.570	0.002	1.0
Dacosta UV response via ERCC3 TTD down	1.547	0.005	1.0	Qi Hypoxia targets of HIF1A and FOXA2	-1.569	0.002	0.870
PID AR pathway	1.547	0.010	1.0	Delpeuch FOXO3 targets up	-1.565	0.007	0.768
Zhan Multiple myeloma HP up	1.518	0.011	1.0	Martinez Response to trabectedin up	-1.564	0.003	0.658
Hedenfalk Breast cancer BRACX down	1.508	0.011	1.0	Tang Senescence TP53 targets down	-1.561	0.007	0.595
PID EPHA2 FWD pathway	1.501	0.015	1.0	Turashvili Breast ductal carcinoma vs lobular normal down	-1.549	0.002	0.691
KEGG Valine, leucine, and isoleucine degradation	1.501	0.024	1.0	Zhong Secretome of lung cancer and fibroblast	-1.548	0.003	0.638
Biocarta MAPK pathway	1.501	0.008	1.0	Korkola Seminoma up	-1.546	0.002	0.599
Nikolsky Breast cancer 8P12 P11 amplicon	1.498	0.034	1.0	Mense Hypoxia up	-1.540	0.008	0.625
Reactome TCR signalling	1.490	0.013	1.0	PID Integrin A4B1 pathway	-1.539	0.004	0.585
Yokoe Cancer testis antigens	1.489	0.026	1.0	Winter Hypoxia metagene	-1.535	0.003	0.598
KEGG Notch signalling pathway	1.488	0.019	1.0	Brideau Imprinted genes	-1.533	0.002	0.573
Huttmann B CLL poor survival down	1.487	0.025	1.0	Rodwell Ageing kidney no blood up	-1.532	0.002	0.544
PID Aurora A pathway	1.483	0.024	1.0	Naba Matrisome	-1.525	0.000	0.601
KEGG Colorectal cancer	1.476	0.034	1.0	Sweet KRAS targets down	-1.524	0.007	0.580
Smirnov Response to IR 2HR up	1.470	0.026	1.0	Reactome Eukaryotic translation elongation	-1.519	0.010	0.604
Lee Liver cancer ACOX1 down	1.462	0.028	1.0	Rizki Tumour invasiveness 2D down	-1.514	0.009	0.638
Madan DPPA4 targets	1.462	0.036	1.0	Nikolsky Breast cancer 20Q12 Q13 amplicon	-1.514	0.005	0.606

Supplementary Figure 7: **RNAseq and gene set enrichment analysis of genes differentially expressed in 8226.CR compared to 8226.wt**. **A**) RNA-sequencing was performed on drug-naïve RPMI-8226 (8226.wt) cells and carfilzomib-resistant RPMI-8226 (8226.CR) cells, with the heat map showing changes in gene expression of at least two-fold between these cell line. **B**) Gene set enrichment analysis of differentially regulated genes in 8226.CR cells compared to 8226.wt cells was conducted, with the top twenty upregulated and downregulated pathways shown, with further details shown in panel (**C**), including the full name of the gene set according to the C2 collection of the Molecular Signature Database, the normalised enrichment score (NES), the nominal p-value, and the false discovery rate (FDR) q-value.

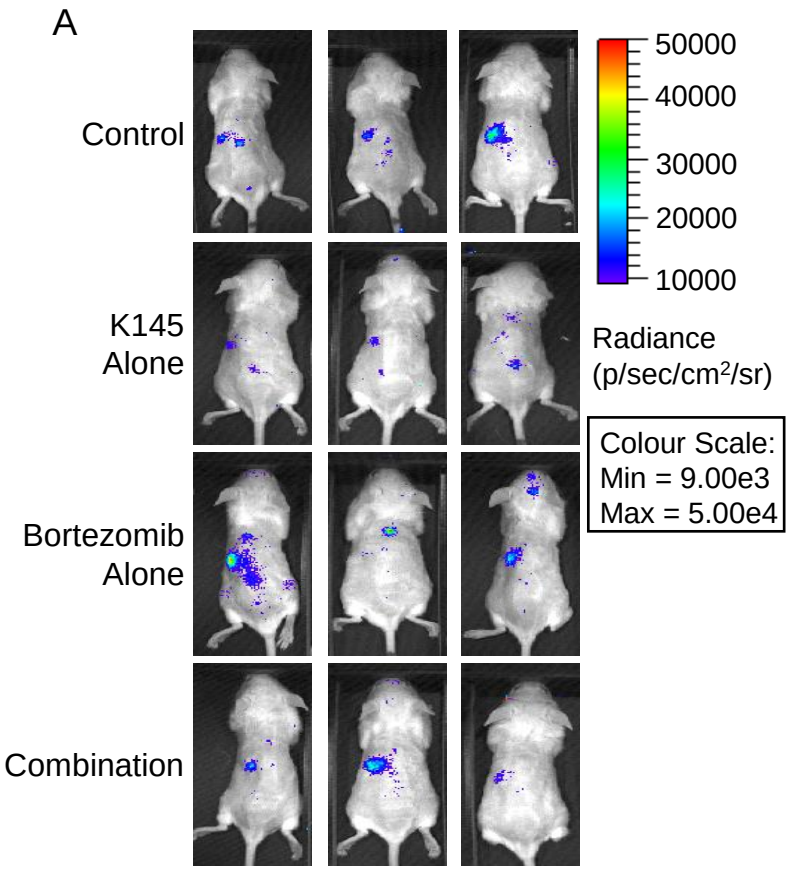

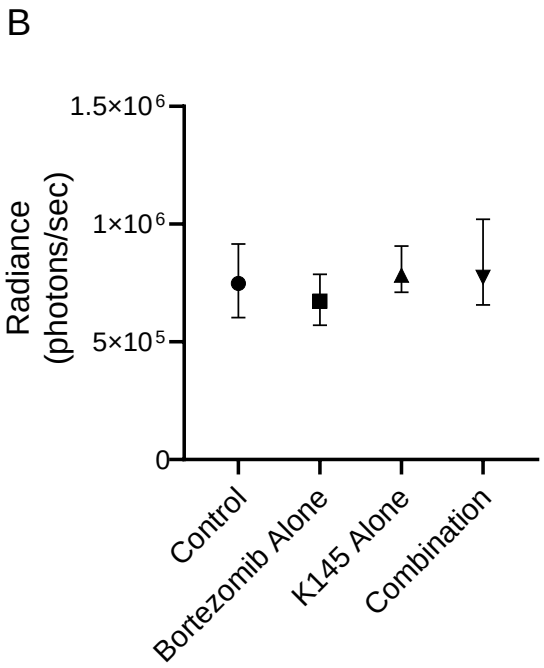

Supplementary Figure 8: **Disease burden in mouse myeloma model prior to treatment. A**) The same representative mice from Figure 6, showing disease burden directly before treatment (14 days post cell injection) at a lower bioluminescence scale. **B)** The median disease burden immediately before treatment (14 days post cell injection) in each treatment group after randomisation, ± 95% confidence interval.

Supplementary Table 1: **Genes differentially regulated in 5TGM1.BR cells compared to 5TGM1.wt cells.** RNAseq was performed on the 5TGM1.BR and 5TGM1.wt cells, with all genes up or downregulated by at least two-fold in 5TGM1.BR cells compared to 5TGM1.wt cells shown. Fold change in 5TGM1.BR cells compared to 5TGM1.wt cells shown in log2 format, along with the p-value and false discovery rate for this fold change. Included at the bottom of the table is the fold change for *PSMB5*, *PSMB6*, and *PSMB7*, none of which appeared to be differentially regulated.

See attached excel table; Bennett et al_Supplementary Table 1

Supplementary Table 2: **Genes likely homozygously mutated in the 5TGM1.BR cells 5TGM1.wt cells.** Variant analysis was conducted on the RNAseq data from the 5TGM1.BR and 5TGM1.wt cells, with the genes that were homozygous wildtype compared to the reference genome in the 5TGM1.wt cells and likely homozygous mutant in the 5TGM1.BR cells shown here. Refence genome used was C57BL_6NJ. Synonymous mutations were excluded

Gene name	Protein name	Gene alteration and location	Protein Alteration
Psmb5	Proteasome subunit beta 5	G→C 14:54616784	Ala→Gly, position 79
Kat7	Lysine acetyltransferase 7	A→G 11:95284027	Splice donor variant, leads to inclusion of pseudo-exon
Rhobtb2	Rho related BTB domain containing 2	C→A 14:69786154	Alteration in 3' UTR
Fbxl3	F-box and leucine rich repeat protein 3	C→G 14:103099308	Alteration in 5' UTR
Cpeb2	Cytoplasmic polyadenlyation element binding protein 2	A→C 5:43278669	Ser→Arg, position 771
Bcat1	Branched chain amino acid transaminase 1	A→C 6:145039454	Val→Gly, position 87
Zbtb33	Zinc finger and BTB domain containing 33	G→A X:38193612	Gly→Ser, position 446

Supplementary Table 3: **Genes differentially regulated in 8226.BR cells compared to 8226.wt cells.** RNAseq was performed on the 8226.BR and 8226.wt cells, with all genes up or downregulated by at least two-fold in 8226.BR cells compared to 8226.wt cells shown. Fold change in 8226.BR cells compared to 8226.wt cells shown in log2 format, along with the p-value and false discovery rate for this fold change.

See attached excel spreadsheet; Bennett et al_Supplementary Table 3

Supplementary Table 4: **Genes likely homozygously mutated in 8226.BR cells compared to 8226.wt.** Genes found in variant analysis of RNAseq data from 8226.wt and 8226.BR to be significant (Fisher exact test p-value<0.01), extremely rare (minor allele frequency<0.05%), and entirely matching the reference genome (hg19) in 8226.wt cells and entirely alternative to the reference genome in 8226.BR cells. Synonymous mutations were excluded.

Gene name	Protein name	Gene alteration and location	Protein Alteration
THEM4	Thioesterase superfamily member 4	G→A 1:151847037	Alteration in 3' UTR
RNF180	Ring finger protein 180	G→C 5:63666570	Alteration in 3' UTR
DPY19L1P1	Dpy-19-like 1 pseudogene 1	G→A 7:32793722	Intron variant
PEX2	Peroxisomal biogenesis factor 2	A→T 8:77895795	Leu→His, position 207
MKI67	Marker of proliferation Ki-67	C→G 10:129913426	Glu→Gln, position 771
STIP1	Stress-induced phosphoprotein 1	G→A 11:63965149	Intron variant
CADM1	Cell adhesion molecule 1	C→G 11:115045831	Alteration in 3' UTR
TIGD7	Tigger transposable element derived protein 7	G→C 16:3349704	Ser→Cys, position 304
DGCR2	DiGeorge syndrome critical region protein 2	C→G 22:19028685	Asp→His, position 428

Supplementary Table 5: **Genes differentially regulated in 8226.CR cells compared to 8226.wt cells.** RNAseq was performed on the 8226.CR and 8226.wt cells, with all genes up or downregulated by at least two-fold in 8226.CR cells compared to 8226.wt cells shown. Fold change in 8226.CR cells compared to 8226.wt cells shown in log2 format, along with the p-value and false discovery rate for this fold change.

See attached excel spreadsheet; Bennett et al_Supplementary Table 5

Supplementary Table 6: **Genes likely homozygously mutated in 8226.CR cells compared to 8226.wt.** Genes found in variant analysis of RNAseq data from 8226.wt and 8226.CR to be significant (Fisher exact test p-value<0.01), extremely rare (minor allele frequency<0.05%), and entirely matching the reference genome (hg19) in 8226.wt cells and entirely alternative to the reference genome in 8226.CR cells. Synonymous mutations were excluded.

Gene name	Protein name	Gene alteration and location	Protein Alteration
DPY19L1P1	Dpy-19-like 1 pseudogene 1	G→A 7:32793722	Intron variant
ADAM8	A disintegrin and metalloproteinase domain 8	C→G 10:135081513	Glu→Gln, position 725
EMP2	Epithelial membrane protein 2	G→A 16:10625854	Alteration in 3’ UTR

Supplementary Table 7**: Genes up or downregulated in all proteasome-inhibitor resistant cell lines**. As shown in Figure 4A, there were only 26 genes found to be up or downregulated in 5TGM1.BR, 8226.BR and 8226.CR compared to their drug-naïve controls. Both the human gene and the mouse analogue are given, along with the fold change in log2 format, the p-value and the false discovery rate for these genes in all three cell lines.

Human gene	Mouse analogue	Fold change (log2)			P-value			FDR		
		5TGM1.BR	8226.BR	8226.CR	5TGM1.BR	8226.BR	8226.CR	5TGM1.BR	8226.BR	8226.CR
TMOD1	Tmod1	2.683	4.552	1.297	1.61E-113	6.02E-146	1.51E-06	7.87E-112	7.35E-145	3.34E-06
TEX19	Tex19.2	1.030	1.476	2.303	1.66E-19	5.87E-51	6.97E-149	1.03E-18	3.17E-50	1.41E-147
SEMA4F	Sema4f	1.265	5.316	4.974	3.95E-13	1.56E-197	8.26E-169	1.67E-12	2.79E-196	1.86E-167
PTPN22	Ptpn22	2.873	3.711	3.697	0	0	0	0	0	0
PLEKHG4	Plekhg4	1.147	2.124	1.911	1.89E-16	7.61E-101	3.69E-83	9.81E-16	6.89E-100	4.60E-82
KSR1	Ksr1	1.145	2.218	1.885	1.14E-35	4.29E-79	3.97E-58	1.30E-34	3.21E-78	3.81E-57
HLA-DMB	H2-DMb1	1.383	3.683	1.189	1.46E-153	3.75E-175	2.29E-12	1.22E-151	5.63E-174	7.30E-12
DCLK2	Dclk2	1.055	1.775	1.095	4.43E-72	6.47E-53	4.37E-20	1.19E-70	3.58E-52	1.95E-19
CMYA5	Cmya5	1.521	1.581	1.063	6.54E-55	2.26E-34	4.14E-16	1.26E-53	9.23E-34	1.57E-15
ANKRD55	Ankrd55	1.182	6.626	6.132	3.68E-53	0	0	6.68E-52	0	0
TNS1	Tns1	-2.744	-5.061	-2.077	1.03E-56	7.79E-131	6.41E-51	2.07E-55	8.66E-130	5.65E-50
TNNT1	Tnnt1	-1.532	-6.762	-4.995	3.38E-45	6.32E-184	2.54E-197	4.98E-44	1.02E-182	6.71E-196
SLC2A3	Slc2a3	-2.529	-4.154	-4.420	4.47E-146	3.09E-268	0	3.44E-144	8.15E-267	0
SLA	Sla	-1.468	-8.976	-1.937	1.40E-226	1.47E-318	1.46E-94	1.99E-224	5.07E-317	1.99E-93
PIM2	Pim2	-1.263	-1.289	-1.429	1.89E-177	6.05E-127	5.19E-155	1.96E-175	6.57E-126	1.09E-153
P2RY10	P2ry10	-4.506	-3.849	-3.712	1.27E-116	2.31E-115	1.48E-135	6.60E-115	2.32E-114	2.74E-134
MYO10	Myo10	-1.181	-14.617	-4.497	1.30E-27	0	0	1.13E-26	0	0
JAKMIP2	Jakmip2	-2.067	-10.553	-7.226	2.19E-53	0	0	4.02E-52	0	0
IFITM1	Ifitm2	-1.296	-2.926	-4.746	1.07E-24	2.59E-154	4.7E-300	8.37E-24	3.38E-153	2.16E-298
HIST1H2BD	Hist3h2ba	-1.003	-1.535	-1.472	4.80E-60	1.22E-24	9.08E-24	1.02E-58	4.02E-24	4.52E-23
HIST1H1C	Hist1h1c	-1.237	-1.315	-2.188	6.33E-99	1.45E-47	6.13E-121	2.53E-97	7.43E-47	1.01E-119
ESRP1	Esrp1	-1.457	-10.397	-1.343	1.96E-15	0	1.22E-80	9.63E-15	0	1.48E-79
BMP1	Bmp1	-1.142	-1.926	-1.088	8.22E-93	5.61E-135	6.59E-56	2.98E-91	6.44E-134	6.16E-55
ALDOC	Aldoc	-4.787	-1.020	-1.667	0	3.13E-54	1.26E-137	0	1.76E-53	2.36E-136
ADAM11	Adam11	-3.229	-1.960	-2.774	4.92E-39	7.73E-50	2.55E-92	6.19E-38	4.1E-49	3.42E-91
ACPP	Acpp	-1.702	-1.831	-2.470	6.13E-33	8.67E-73	9.15E-127	6.42E-32	6.09E-72	1.59E-125